

Q-scan-analysis of the neutron scattering in iron-based superconductors

Yuki Nagai^{1,2,3} and Kazuhiko Kuroki^{4,3}

¹CCSE, Japan Atomic Energy Agency, 5-1-5 Kashiwanoha, Kashiwa, Chiba, 277-8587, Japan

²CREST(JST), 4-1-8 Honcho, Kawaguchi, Saitama, 332-0012, Japan

³TRIP(JST), Chiyoda, Tokyo 102-0075, Japan

⁴Department of Applied Physics and Chemistry, The University of Electro-Communications, Chofu, Tokyo 182-8585, Japan

(Dated: September 15, 2018)

We propose a way to determine the pairing state of the iron pnictide superconductors exploiting the momentum (Q) scan of the neutron scattering data. We investigate the spin susceptibility in the s_{\pm} and s_{++} superconducting states for various doping levels using the effective five-orbital model and considering the quasiparticle damping. The peak position of the intensity shifts from the position on the line $Q_x = \pi$ to that on the line $Q_y = 0$ as the doping level is decreased from electron doping to hole doping. We find that the Q -dependence of the ratio of the intensity in the superconducting state to that in the normal state is qualitatively different between the s_{\pm} -wave and s_{++} -wave pairings. We propose to investigate experimentally this ratio in Q -space to distinguish the two pairing states.

PACS numbers: 74.20.Rp, 78.70.Nx, 74.70.Xa

I. INTRODUCTION

The discovery of the iron-based superconductors has attracted considerable attention because of the high superconducting transition temperature¹. The possibility of a peculiar unconventional pairing state has also been an issue of great interest. In fact, spin-fluctuation-mediated s_{\pm} -wave pairing state has been proposed at the early stage of the study²⁻⁷, where the superconducting gap is fully open, but changes its sign across the wave vector that bridges the disconnected Fermi surfaces. The sign change occurs because repulsive pairing interaction arises from the spin fluctuations that develop around the Fermi surface nesting vector.

There are many experimental results which suggest that the order parameter is fully gapped in a number of iron-based superconductors, such as the penetration depth measurements⁸⁻¹⁰, the angle resolved photoemission spectroscopy¹¹⁻¹³, and the scanning tunneling microscopy/spectroscopy (STM/STS)¹⁴. There are also experimental suggestions that the superconducting gap has an unconventional form with sign change. The nuclear magnetic relaxation rate lacks the coherence peak below T_c ¹⁵⁻¹⁸, which suggests that there is a sign change in the order parameter. In addition, integer and half-integer flux-quantum transitions in composite niobium-iron pnictide loops have also been observed¹⁹, which again suggests the presence of the sign change in the order parameter. In Ref. 14, STM/STS measurements have been performed to detect the quasiparticle interference originating from the s_{\pm} -gap. These experiments seem to be consistent with the s_{\pm} -wave pairing scenario.

On the other hand, there has been a debate concerning the sensitivity of T_c against impurities. There have been a number of studies regarding the issue of whether the pairing state in the iron pnictides is robust against impurities or not²⁰⁻²³. It has been pointed out that the suppression of T_c by impurities is too weak for a pair-

ing state with a sign change in the gap in some papers e.g., Ref. 23. A calculation based on a five-band model by Onari *et al.* has supported this theoretically²⁵, although the strength of the impurity potential adopted there is large compared to those calculated from first principles²⁶. As a possible pairing state that is robust against impurities, the so-called s_{++} -state, where the gap does not change its sign between the Fermi surfaces, has been proposed²⁷⁻²⁹.

As for the probe to determine the pairing state, it has been proposed at the early stage^{5,30,31} that the observation of neutron scattering resonance at the nesting vector of the electron and hole Fermi surfaces is one of the useful ways to determine whether there is sign change of the gap between these disconnected Fermi surfaces. In fact, neutron scattering experiments have observed a peak-like structure in the superconducting state³²⁻³⁷. This has been taken as strong evidence for the sign change in the superconducting gap. On the other hand, Onari *et al.* later took into account the quasiparticle damping effect in the calculation of the dynamical spin susceptibility, and showed that a peak-like enhancement over the normal state values can be obtained even in the s_{++} state, which is due to the suppression of the normal state susceptibility originating from the damping^{38,39}. In these studies, they claim that the enhancement that originates from the resonance of the s_{\pm} -wave pairing is too strong to explain the experimental observations, and the 'hump-like structure' of the intensity in the s_{++} -wave pairing is more likely to be the origin. However, a quantitative comparison between theories and experiments should actually be very difficult since there are many parameters that can affect the intensity, e.g., the doping-level, the band-structure, the strength of the electron interaction, and among all, the adopted theoretical method (random phase approximation, fluctuation exchange, etc.) Therefore, we need to look for a more qualitative difference between the peak structures in the two pairing states,

which can be understood intuitively. Recently, we have proposed to investigate experimentally the wave vector $\sim (\pi, \pi)$ in the unfolded Brillouin zone, in addition to the usually considered $\sim (\pi, 0)/(0, \pi)$, to distinguish the two pairing states qualitatively⁴⁰. In this paper, we extend this study, and obtain a \mathbf{Q} (momentum)- E (energy) scan of the dynamical susceptibility. The momentum is scanned along the whole symmetric lines. We also investigate the doping concentration dependence, where a recent experimental as well as theoretical studies in the normal state have revealed an electron-hole asymmetry of the incommensurability of the spin fluctuation^{44,45}. We propose that by looking at the superconducting to normal state ratio of the dynamical susceptibility, the two states give qualitative difference reflecting the difference in the mechanism of the occurrence of the peak like structure. The ratio is barely momentum dependent in the s_{++} state, while in the s_{\pm} state it is maximized around the wave vector at which the normal spin susceptibility is maximized.

This paper is organized as follows. In Sec. II, four effective models for electron- or hole-doped systems and the formulation of the spin susceptibility are presented. We introduce the multi-orbital random phase approximation (RPA) with the quasiparticle damping. In Sec. III, the calculation results are presented. We systematically investigate the doping-level and scattering vector dependences, and point out a qualitative difference between s_{\pm} -wave and s_{++} -wave states. In Sec. IV, the conclusion is given.

II. FORMULATION

A. The effective models

We introduce two-dimensional five-orbital models of 1111 materials obtained in the unfolded Brillouin zone⁷, where the x - and y - axes are taken in the Fe-Fe bond direction. To investigate the doping-level dependence, we consider four situations : lightly electron-doped (the band filling $n \sim 6.04$), optimally electron-doped ($n \sim 6.1$), heavily-electron doped (the band filling is $n \sim 6.3$), optimally hole-doped ($n \sim 5.8$) cases. For the electron doped cases, we use the model of LaFeAsO, while for the hole doped case, to mimic the band structure of the 122 materials, where the xy hole Fermi surface around the wave vector (π, π) in the unfolded Brillouin zone is robust, we use a two dimensional model of NdFeAsO⁴³. This is just for simplicity in the calculation, namely, the model of the 122 systems have strong three dimensionality, which is difficult to cope with within the present formalism. We expect that the three dimensionality itself does not affect the conclusion of the present study. The Fermi surfaces of each dopings are shown in Fig. 1.

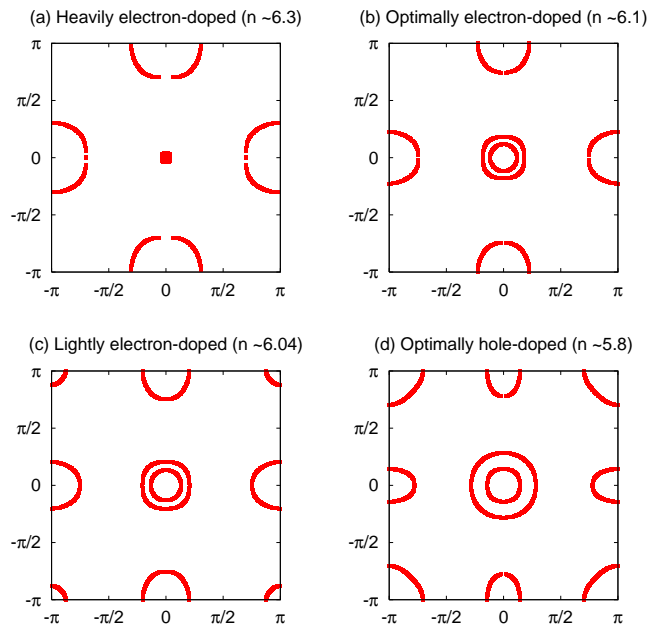


FIG. 1. Fermi surfaces for (a) heavily electron-doped ($n \sim 6.3$), (b) optimally electron-doped ($n \sim 6.1$), (c) lightly electron-doped ($n \sim 6.04$), and (d) optimally hole-doped ($n \sim 5.8$) cases.

B. Spin susceptibility

The dynamical spin susceptibility is given by

$$\chi(\mathbf{Q}, E) = \sum_{a,c} \chi_{cc}^{aa}(\mathbf{Q}, E). \quad (1)$$

Here, $\chi_{cc}^{aa}(\mathbf{Q}, E)$ denotes an orbital-dependent spin susceptibility. The inelastic neutron scattering intensity is proportional to $\chi''(\mathbf{Q}, E)$ which is the imaginary part of $\chi(\mathbf{Q}, E)$. In the multi-orbital RPA, an orbital-dependent spin susceptibility $\chi_{cc}^{aa}(\mathbf{Q}, E)$ is written as

$$\chi_{cc}^{aa}(\mathbf{Q}, E) = \left[(\hat{1} - \hat{\chi}_0(\mathbf{Q}, E) \hat{U}_s)^{-1} \hat{\chi}_0(\mathbf{Q}, E) \right]_{cc}^{aa}, \quad (2)$$

where $\hat{\chi}_0(\mathbf{Q}, E)$ is the bare spin susceptibility expressed as

$$\begin{aligned} [\chi_0(\mathbf{Q}, E)]_{cd}^{ab} = & - \sum_{\mathbf{k}} \sum_{\nu\nu'} \left[M_{abcd}^{\nu\nu'G}(\mathbf{k}, \mathbf{k} + \mathbf{Q}) \chi_{0G}^{\nu\mu}(\mathbf{k}, \mathbf{k} + \mathbf{Q}, E) \right. \\ & \left. + M_{abcd}^{\nu\nu'F}(\mathbf{k}, \mathbf{k} + \mathbf{Q}) \chi_{0F}^{\nu\nu'}(\mathbf{k}, \mathbf{k} + \mathbf{Q}, E) \right]. \end{aligned} \quad (3)$$

Here, $\chi_{0G(F)}^{\nu\nu'}(\mathbf{k}, \mathbf{k} + \mathbf{Q}, E)$ denotes the normal (anomalous) part of the band-dependent BCS spin susceptibility

written as

$$\chi_{0G}^{\nu\nu'}(\mathbf{k}, \mathbf{k} + \mathbf{Q}, E) = \frac{|v_{\mathbf{k}}^{\nu'}|^2 |u_{\mathbf{k}+\mathbf{Q}}^{\nu'}|^2}{E + i\Gamma_{\mathbf{k},\mathbf{q}}^{\nu\nu'} - E_{\mathbf{k}+\mathbf{Q}}^{\nu'} - E_{\mathbf{k}}^{\nu}} \quad (4)$$

$$\chi_{0F}^{\nu\nu'}(\mathbf{k}, \mathbf{k} + \mathbf{Q}, E) = -\frac{u_{\mathbf{k}}^{\nu*} v_{\mathbf{k}}^{\nu'} u_{\mathbf{k}+\mathbf{q}}^{\nu'} v_{\mathbf{k}+\mathbf{Q}}^{\nu'*}}{E + i\Gamma_{\mathbf{k},\mathbf{q}}^{\nu\nu'} - E_{\mathbf{k}+\mathbf{Q}}^{\nu'} - E_{\mathbf{k}}^{\nu}}, \quad (5)$$

at zero-temperature ($E > 0$) with $E_{\mathbf{k}}^{\nu} = \sqrt{\epsilon_{\mathbf{k}}^{\nu 2} + |\Delta_{\mathbf{k}}^{\nu}|^2}$, $|u_{\mathbf{k}}^{\nu}|^2 = (1 + \epsilon_{\mathbf{k}}^{\nu}/E_{\mathbf{k}}^{\nu})/2$, $|v_{\mathbf{k}}^{\nu}|^2 = (1 - \epsilon_{\mathbf{k}}^{\nu}/E_{\mathbf{k}}^{\nu})/2$, $u_{\mathbf{k}}^{\nu} v_{\mathbf{k}}^{\nu*} = \Delta_{\mathbf{k}}^{\nu}/(2E_{\mathbf{k}}^{\nu})$, and $\epsilon_{\mathbf{k}}^{\nu}$ is the ν -th band energy measured relative to the Fermi energy. $M_{abcd}^{\nu\nu'G}(\mathbf{k}, \mathbf{k} + \mathbf{Q})$ ($M_{abcd}^{\nu\nu'F}(\mathbf{k}, \mathbf{k} + \mathbf{Q})$) is given by

$$M_{abcd}^{\nu\nu'G}(\mathbf{k}, \mathbf{k} + \mathbf{Q}) = U_{a\nu}^*(\mathbf{k}) U_{b\nu'}(\mathbf{k} + \mathbf{Q}) U_{c\nu'}^*(\mathbf{k} + \mathbf{Q}) U_{d\nu}(\mathbf{k}), \quad (6)$$

$$M_{abcd}^{\nu\nu'F}(\mathbf{k}, \mathbf{k} + \mathbf{Q}) = U_{a\nu}^*(\mathbf{k}) U_{b\nu'}(\mathbf{k} + \mathbf{Q}) U_{c\nu}(\mathbf{k}) U_{d\nu'}^*(\mathbf{k} + \mathbf{Q}), \quad (7)$$

with the unitary matrix $\check{U}(\mathbf{k})$ which diagonalizes the Hamiltonian in the orbital basis. Here, we introduce the band-index ν whose energy $\epsilon_{\mathbf{k}}^{\nu}$ satisfies the relation $\epsilon_{\mathbf{k}}^{\nu} > \epsilon_{\mathbf{k}}^{\nu'}$ ($\nu > \nu'$). For the ' s_{++} -wave', we take $\Delta^2 = \Delta^3 = \Delta^4 = \Delta_0$ and for ' s_{\pm} -wave' $\Delta^2 = \Delta^3 = -\Delta^4 = \Delta_0$. As done in Ref. 31, we introduce a Gaussian cutoff for the gap $\Delta_{\mathbf{k}}^{\nu} = \Delta^{\nu} \exp\{-[\epsilon_{\mathbf{k}}^{\nu}/\Delta E]^2\}$, and take $\Delta E = 4\Delta_0$.

We employ the orbital dependent interactions in the form $\check{U}_s = a\check{U}_{\text{Miyake}}$. Here, $\check{U}_{\text{Miyake}}$ are the orbital dependent interactions obtained from the first-principles calculation by Miyake *et al.*⁴² In the RPA calculation, since realistic values of the interaction results in very large spin fluctuations, we multiply all the electron-electron interaction by a reduction factor a . We set $a = 0.5$ for $n \sim 6.1$, $a = 0.45$ for $n \sim 6.04$, $a = 0.55$ for $n \sim 6.3$, and $a = 0.4$ for $n \sim 5.8$. These values of a are close to the maximum value that can be adopted in the present formalism (larger values give magnetic transition), which is dependent on the band filling. The variance of the maximum value of a is actually largely due to the approximation adopted here (RPA), where the self energy corrections are not taken into account. Nevertheless, we have confirmed that our results do not change qualitatively if we take other values of the reduction factor.

We consider the quasiparticle damping $\Gamma_{\mathbf{k},\mathbf{q}}^{\nu\nu'}$ in the form

$$\Gamma_{\mathbf{k},\mathbf{q}}^{\nu\nu'} = \max(\gamma_{\mathbf{k}}^{\nu}, \gamma_{\mathbf{k}+\mathbf{q}}^{\nu'}), \quad (8)$$

where

$$\gamma_{\mathbf{k}}^{\nu} = \begin{cases} \eta & (|E_{\mathbf{k}}^{\nu}| < 3|\Delta_{\mathbf{k}}^{\nu}|) \\ \gamma_0 & (4|\Delta_{\mathbf{k}}^{\nu}| < |E_{\mathbf{k}}^{\nu}|) \\ (\gamma_0 - \eta) \frac{|E_{\mathbf{k}}^{\nu}|}{|\Delta_{\mathbf{k}}^{\nu}|} - 3(\gamma_0 - \eta) + \eta & (\text{else}) \end{cases}. \quad (9)$$

This form of the damping was introduced in Ref. 38 from the requirement that the damping should not be present in the low energy regime of less than 3Δ , which is equal to the particle-hole excitation gap plus one-particle gap.

In the high energy regime, the damping should be essentially the same as that in the normal state, and the present form interpolates the low and high energy regimes in a simple manner. To be more strict, the damping of the superconducting state in the high energy regime can be different from that in the normal state above T_c because the temperature is different. However, it is known experimentally that the dynamical susceptibility in the normal and the superconducting states nearly coincide with each other in the high energy regime³⁴, indicating that the temperature dependence of the damping in the high energy regime is not so strong. Therefore, we take the same value of γ_0 for the normal and the superconducting states. Although we use this specific form of the damping in the actual calculation, the present results are not qualitatively dependent on the details of the damping.

III. RESULTS

We investigate the \mathbf{Q} - E map of the spin susceptibility $\chi''(\mathbf{Q}, E)$. Since the commensurate vector is $\mathbf{Q} = (\pi, 0)$, we calculate \mathbf{Q} -dependence along two lines in \mathbf{Q} -map. One is the line on the Q_x -axis, i.e., $\mathbf{Q} = (Q_x, 0)$, and the other is the line with $Q_x = \pi$, $\mathbf{Q} = (\pi, Q_y)$. In this paper, the smearing factor and the magnitude of the superconducting gap are taken to be $\eta = 0.5$ meV, $\Delta_0 = 10$ meV, respectively. We take the quasiparticle damping in the normal state as $\gamma_0 = 10$ meV, which was estimated from the temperature dependence of the resistivity observed experimentally³⁸. To cope with the realistic magnitude of the superconducting gap, we take 4096×4096 \mathbf{k} -point meshes throughout the paper.

First, we will show the results in the normal state to see the peak position of the spin susceptibility. The incommensurability is found to be asymmetric between electron and hole doped cases, as was found experimentally⁴⁴ as well as theoretically^{45,46}. Then, we will present the results in the superconducting state to investigate the difference between s_{\pm} -wave and s_{++} -wave states in \mathbf{Q} -maps. We find that the \mathbf{Q} -map of the superconducting/normal ratio is qualitatively different between the two states.

A. Normal state

We show the results in the normal state in Fig. 2. We find that the peak position of the intensity shifts from the position on the line $Q_x = \pi$ to that on the line $Q_y = 0$ as we decrease the electron doping level, and go into the hole doping regime (see Fig. 3). This electron-hole asymmetry of the incommensurability of the spin fluctuations has been attributed to the multiorbital nature of the Fermi surface^{44,45}. It should also be noted in the heavily electron doped regime of $n = 6.3$, the incommensurability is very large, coming somewhat close to $(\pi/2, \pi)$. This structure comes partially from the interaction between

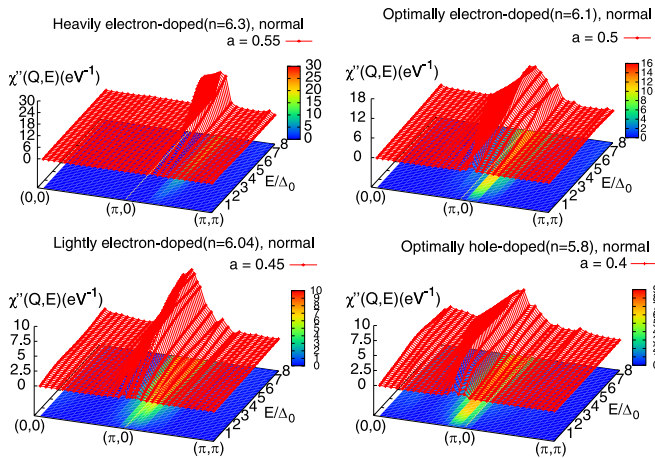


FIG. 2. Q - E map of the spin susceptibility $\chi''(\mathbf{Q}, E)$ in the normal state for heavily electron-doped (the band filling is $n \sim 6.3$), optimally electron-doped ($n \sim 6.1$), lightly electron-doped ($n \sim 6.04$), and optimally hole-doped ($n \sim 5.8$) cases.

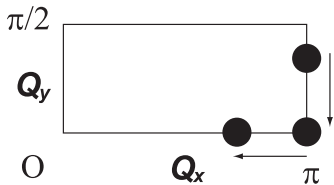


FIG. 3. Schematic figure of the peak-position shift in Q -space with decreasing the doping level.

two electron pockets^{7,43}, but there turns out to be also a contribution from the interaction between the electron and the barely present hole Fermi surfaces (as we shall see more clearly in the superconducting state), which are not well nested at this doping level. In this sense, we are using the term “nesting” in a rather broad sense of the term. Another point to be noted in the heavily electron doped regime ($n = 6.3$) is the absence of intensity at low energies, which reflects the fact that the hole Fermi surfaces are barely present. As for the interaction strength dependence, we have confirmed that the peak position does not depend on the interaction reducing factor a .

B. Superconducting state: s_{\pm} -wave pairing

Let us now consider the superconducting state with s_{\pm} -wave pairing. We show the Q - E maps of the spin susceptibility $\chi''(\mathbf{Q}, E)$ in Fig. 4. We can clearly see the shift of the peak position with decreasing the doping level, i.e., the resonance peak moves in accord with the normal state peak position. It should be noted that the peak intensity also depends on the doping level as well as the interaction strength. For example, the peak at the incommensurate vector $\mathbf{Q} = (\pi, \pi/8)$ for the optimally

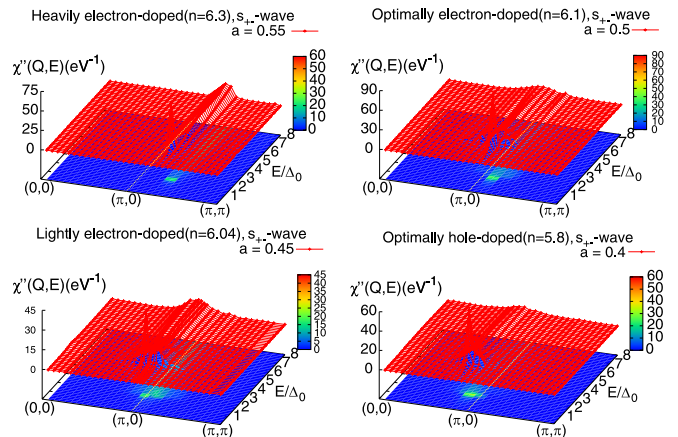


FIG. 4. Q - E map of the spin susceptibility $\chi''(\mathbf{Q}, E)$ in the s_{\pm} -wave pairing state for the four band filling cases.

electron-doped case ($n \sim 6.1$) gives the largest peak intensity among these four doping levels. Therefore, we point out once again that it is difficult to determine the pairing state from quantitative comparison between experiments and theory since the peak intensity depends on the doping level n as well as the strength of the electron interaction \hat{U}_s . Another point that should be noted here is that the resonance peak exists in the heavily electron doped regime $n = 6.3$, reflecting the sign change of the gap between electron and hole Fermi surfaces. This means that there is a certain contribution to the structure close to $(\pi, \pi/2)$ also from the “badly nested” electron and hole Fermi surfaces, as mentioned in the section for the normal state. A resonance at a wave vector close to $(\pi, \pi/2)$ in heavily overdoped systems, as is observed for instance in Ref.⁴⁷, is interpreted as a signature of d -wave pairing⁴⁸ where the gap sign changes between electron pockets, but the present study suggests that it may also be interpreted in terms of s_{\pm} pairing originating from badly nested electron and hole pockets⁴⁹.

C. Superconducting state: s_{++} -wave pairing

Next, we consider the s_{++} -wave state. We show the Q - E maps of the spin susceptibility $\chi''(\mathbf{Q}, E)$ in Figs. 5. As pointed out previously^{38,40}, the quasiparticle damping makes the hump structure in the s_{++} -wave pairing state. The hump structure moves as the doping level is varied, which at first sight may look similar to that in the s_{\pm} state. However, there is a large difference between these two states, which is revealed by taking the ratio between the normal and the superconducting states.

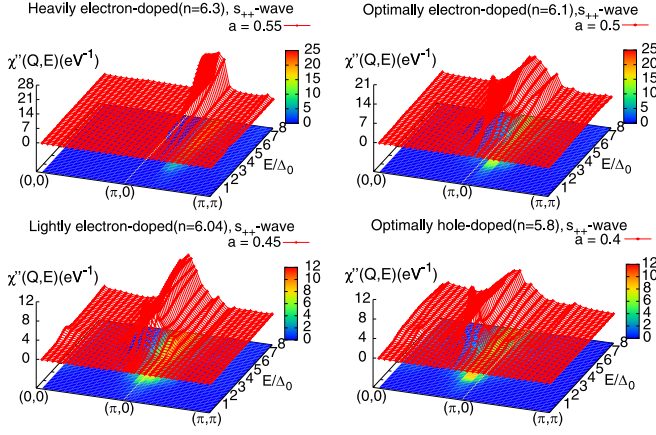


FIG. 5. Q - E map of the spin susceptibility $\chi''(\mathbf{Q}, E)$ in the s_{++} -wave pairing state for the four band filling cases.

D. Superconducting to normal ratio

We now show the Q - E map of the ratio of the spin susceptibility in the superconducting state to that in the normal state in Figs. 6. As shown in the left panels in these figures, the ratio becomes large in a localized regime around $\mathbf{Q} \sim (\pi, 0)$ in the case of the s_{\pm} -wave pairing. To be more precise, one can find in Fig. 7 that the peak position of the ratio in the low energy region ($E < 2\Delta_0$) shifts with decreasing the doping level, in accord with the peak position of the spin susceptibility in the normal state as was shown in Fig. 3. By contrast, in the case of s_{++} -wave pairing, we find that the ratio is weakly dependent on \mathbf{Q} as shown in the lower panels in Fig. 6. This is a qualitative difference between the s_{\pm} -wave and s_{++} -wave pairing.

The above difference originates from the difference of the mechanism of the enhancement between the two cases. In the s_{\pm} -wave pairing state, the enhancement originates from the sign change of the gap across the wave vector that bridges the Fermi surface, so that the maximum value of the ratio in \mathbf{Q} -space is localized around this wave vector. On the other hand, in the s_{++} -wave pairing state, the enhancement comes from the quasiparticle damping effect, which is not momentum dependent. As pointed out in previous studies^{39,40}, the dissipation increases in the high energy region ($E > 3\Delta_0$) is the origin of the decrease of the intensity in the high energy region, so that one can see the hump structure as shown in Fig. 5 in the mid-range energy region ($2\Delta_0 < E < 3\Delta_0$). This means that the enhancement (the superconducting to normal ratio) in the s_{++} -wave state and the nesting vector are not related. This was the original motivation for the proposal to investigate experimentally the wave vector $\sim (\pi, \pi)$ to distinguish between two cases⁴⁰. In the present study, it can be more clearly seen that the ratio of the enhancement in the s_{++} -wave state depends weakly on the wave vector. In addition, we also point out

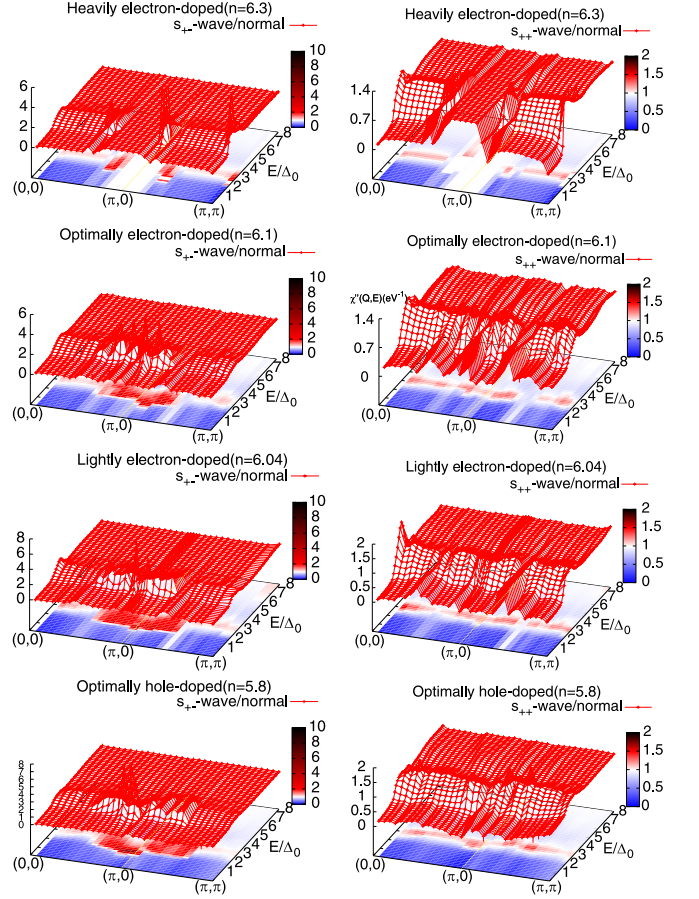


FIG. 6. Q - E map of the ratio of the intensity in the superconducting state to that in the normal state for the four band filling cases. Left panel: the result of the s_{\pm} -wave pairing state. Right panel: the result of the s_{++} -wave pairing state.

that this ratio does not depend on the doping level. This result is easily understood by the nature of the quasiparticle damping. Thus, if the experimentally observed peak structure is coming from the quasiparticle damping, the enhancement ratio of the intensity in the superconducting state to that in normal state has to be weakly momentum dependent. This conclusion is valid in various kinds of the iron-based superconductors.

IV. CONCLUSION

In conclusion, we have obtained the Q -map of the spin susceptibility in the s_{\pm} and s_{++} superconducting states of the iron-based superconductors by applying multiorbital RPA to the effective five-orbital models and considering the quasiparticle damping. We have shown that the peak position of the intensity shifts from the position on the line $Q_x = \pi$ to that on the line $Q_y = 0$ with decreasing the doping level. Considering the difficulty in quantitatively comparing the theories with the

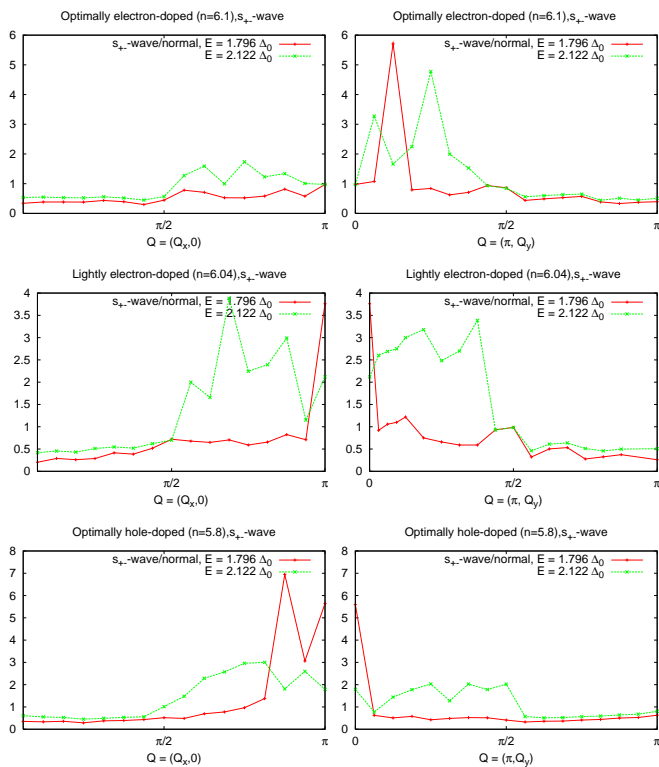


FIG. 7. Q -dependence of the $\chi''(Q, E)$ in the s_{\pm} -wave pairing state. Left panel: Q_x -dependence $Q = (Q_x, 0)$. Right panel: Q_y -dependence $Q = (\pi, Q_y)$.

experiments, we have proposed that the comparison of the Q -dependence of the superconducting to normal ratio of the spin susceptibility is useful in determining the pairing state. In the s_{\pm} -wave state, the ratio is peaked around the nesting vector, and it is dependent on the doping level, while in the s_{++} -wave pairing state, the ratio is weakly dependent on the wave vector. Exploiting the present proposal, we expect that one can distinguish the two pairing states.

ACKNOWLEDGMENT

We thank M. Machida, N. Nakai, Y. Ota, for helpful discussions and comments. The calculations have been performed using the supercomputing system PRIMERGY BX900 at the Japan Atomic Energy Agency.

- ¹ Y. Kamihara, T. Watanabe, M. Hirano, and H. Hosono, *J. Am. Chem. Soc.* **130**, 3296 (2008).
- ² Y. Bang, and H.-Y. Choi, *Phys. Rev. B*, **78**, 134523 (2008).
- ³ K. Seo, B. A. Bernevig, and J. Hu, *Phys. Rev. Lett.* **101**, 206404 (2008).
- ⁴ M. M. Parish, J. Hu, and B. A. Bernevig, *Phys. Rev. B* **78**, 144514 (2008).
- ⁵ M. M. Korshunov and I. Eremin, *Phys. Rev. B* **78**, 140509(R) (2008).
- ⁶ I. I. Mazin, D. J. Singh, M. D. Johannes, and M. H. Du, *Phys. Rev. Lett.* **101**, 057003 (2008).
- ⁷ K. Kuroki, R. Arita, H. Usui, Y. Tanaka, H. Kontani, and H. Aoki, *Phys. Rev. Lett.* **101**, 087004 (2008).
- ⁸ K. Hashimoto, T. Shibauchi, T. Kato, K. Ikada, R. Okazaki, H. Shishido, M. Ishikado, H. Kito, A. Iyo, H. Eisaki, S. Shimoto, and Y. Matsuda, *Phys. Rev. Lett.* **102**, 017002 (2009).
- ⁹ H. Luetkens, H.-H. Klauss, R. Khasanov, A. Amato, R. Klingeler, I. Hellmann, N. Leps, A. Kondrat, C. Hess, A. Köhler, G. Behr, J. Werner, and B. Büchner, *Phys. Rev. Lett.* **101**, 097009 (2008).
- ¹⁰ L. Malone, J. D. Fletcher, A. Serafin, A. Carrington, N. D. Zhigadlo, Z. Bukowski, S. Katrych, and J. Karpinski, *Phys. Rev. B* **79**, 140501(R) (2009).
- ¹¹ H. Ding, P. Richard, K. Nakayama, T. Sugawara, T. Arakane, Y. Sekiba, A. Takayama, S. Souma, T. Sato, T. Takahashi, Z. Wang, X. Dai, Z. Fang, G. F. Chen, J. L. Luo, and N. L. Wang, *EuroPhys. Lett.* **83**, 47001 (2008).
- ¹² K. Nakamura, T. Sato, P. Richard, Y.-M. Xu, Y. Sekiba, S. Souma, G. F. Chen, J. L. Luo, N. L. Wang, H. Ding, and T. Takahashi, *EuroPhys. Lett.* **85** 67002 (2009).
- ¹³ D. V. Evtushinsky, D. S. Inosov, V. B. Zabolotnyy, A. Koitzsch, M. Knupfer, B. Buchner, M. S. Viazovska, G. L. Sun, V. Hinkov, A. V. Boris, C. T. Lin, B. Keimer, A. Varykhalov, A. A. Kordyuk, and S. V. Borisenko, *Phys. Rev. B* **79**, 054517 (2009).
- ¹⁴ T. Hanaguri, S. Nittaka, K. Kuroki, and H. Takagi, *Science* **328**, 474 (2010).
- ¹⁵ Y. Nakai, K. Ishida, Y. Kamihara, M. Hirano, and H. Hosono, *J. Phys. Soc. Japan*, **77** 073701 (2008).
- ¹⁶ H.-J. Grafe, D. Paar, G. Lang, N. J. Curro, G. Behr, J. Werner, J. Hamann-Borrero, C. Hess, N. Leps, R. Klingeler, and B. Büchner, *Phys. Rev. Lett.* **101**, 047003 (2008).
- ¹⁷ H. Mukuda, N. Terasaki, H. Kinouchi, M. Yashima, Y. Kitaoka, S. Suzuki, S. Miyasaka, S. Tajima, K. Miyazawa, P. Shirage, H. Kito, H. Eisaki, and A. Iyo, *J. Phys. Soc. Jpn.* **77**, 093704 (2008).
- ¹⁸ N. Terasaki, H. Mukuda, M. Yashima, Y. Kitaoka, K. Miyazawa, P. M. Shirage, H. Kito, H. Eisaki, and A. Iyo, *J. Phys. Soc. Jpn.* **78**, 013701 (2009).
- ¹⁹ C.-T. Chen, C. C. Tsuei, M. B. Ketchen, Z.-A. Ren, and Z. X. Zhao, *Nature Physics* **6**, 260 (2010).

- ²⁰ Y. F. Guo, Y. G. Shi, S. Yu, A. A. Belik, Y. Matsushita, M. Tanaka, Y. Katsuya, K. Kobayashi, I. Nowik, I. Felner, V. P. S. Awana, K. Yamaura, and E. Takayama-Muromachi, *Phys. Rev. B* **82**, 054506 (2010).
- ²¹ Y. Nakajima, T. Taen, Y. Tsuchiya, T. Tamegai, H. Kitamura, and T. Murakami, *Phys. Rev. B* **82**, 220504(R) (2010).
- ²² S. Kitagawa, Y. Nakai, T. Iye, K. Ishida, Y. F. Guo, Y. G. Shi, K. Yamaura, and E. Takayama-Muromachi, *Phys. Rev. B* **83**, 180501(R) (2011).
- ²³ M. Sato, Y. Kobayashi, S. C. Lee, H. Takahashi, E. Satomi, and Y. Miura, *J. Phys. Soc. Jpn.* **79** (2010) 014710.
- ²⁴ Y. K. Li, X. Lin, Q. Tao, C. Wang, T. Zhou, L. J. Li, Q. B. Wang, M. He, G. H. Cao, and Z. A. Xu, *New J. Phys.* **11** 053008 (2009).
- ²⁵ S. Onari and H. Kontani, *Phys. Rev. Lett.* **103** (2009) 177001.
- ²⁶ K. Nakamura, R. Arita, and H. Ikeda, *Phys. Rev. B* **83**, 144512 (2011).
- ²⁷ H. Kontani and S. Onari, *Phys. Rev. Lett.* **104**, 157001 (2010).
- ²⁸ Y. Yanagi, Y. Yamakawa, N. Adachi, and Y. Ono, *J. Phys. Soc. Jpn.* **79**, 123707 (2010).
- ²⁹ T. Saito, S. Onari, and H. Kontani, *Phys. Rev. B* **82** 144510 (2010).
- ³⁰ T.A. Maier and D. J. Scalapino, *Phys. Rev. B* **78**, 020514(R) (2008).
- ³¹ T. A. Maier, S. Graser, D. J. Scalapino, and P. Hirschfeld, *Phys. Rev. B* **79**, 134520 (2009).
- ³² A. D. Christianson, E. A. Goremychkin, R. Osborn, S. Rosenkranz, M. D. Lumsden, C. D. Malliakas, I. S. Todorov, H. Claus, D. Y. Chung, M. G. Kanatzidis, R. I. Bewley and T. Guidi, *Nature* **456** 930 (2008).
- ³³ Y. Qiu, W. Bao, Y. Zhao, C. Broholm, V. Stanev, Z. Tesanovic, Y. C. Gasparovic, S. Chang, J. Hu, B. Qian, M. Fang, and Z. Mao, *Phys. Rev. Lett.* **103** 067008 (2009).
- ³⁴ D. S. Inosov, J. T. Park, P. Bourges, D. L. Sun, Y. Sidis, A. Schneidewind, K. Hradil, D. Haug, C. T. Lin, B. Keimer and V. Hinkov, *Nature Phys.* **6** 178 (2010).
- ³⁵ J. Zhao, L.-P. Regnault, C. Zhang, M. Wang, Z. Li, F. Zhou, Z. Zhao, C. Fang, J. Hu and P. Dai, *Phys. Rev. B* **81**, 180505(R) (2010).
- ³⁶ M. Ishikado, Y. Nagai, K. Kodama, R. Kajimoto, M. Nakamura, Y. Inamura, S. Wakimoto, H. Nakamura, M. Machida, K. Suzuki, H. Usui, K. Kuroki, A. Iyo, H. Eisaki, M. Arai, S. Shamoto, *Phys. Rev. B* **84**, (2011) 144517.
- ³⁷ C. Zhang, M. Wang, H. Luo, M. Wang, M. Liu, J. Zhao, D. L. Abernathy, T. A. Maier, K. Marty, M. D. Lumsden, S. Chi, S. Chang, J. A. Rodriguez-Rivera, J. W. Lynn, Tao Xiang, Jiangping Hu, P. Dai, *Scientific Reports* **1**, 115 (2011).
- ³⁸ S. Onari, H. Kontani, and M. Sato, *Phys. Rev. B* **81** 060504(R) (2010).
- ³⁹ S. Onari, H. Kontani, *Phys. Rev. B* **84**, 144518 (2011).
- ⁴⁰ Y. Nagai, and K. Kuroki, *Phys. Rev. B* **83**, 220516(R) (2011).
- ⁴¹ Y. Nagai, and K. Kuroki, arXiv:1106.2376 (unpublished); S. Onari, and H. Kontani, arXiv:1107.0748 (unpublished).
- ⁴² T. Miyake, K. Nakamura, R. Arita, and M. Imada, *J. Phys. Soc. Jpn.* **79** (2010), 044705.
- ⁴³ K. Kuroki, H. Usui, S. Onari, R. Arita, and H. Aoki, *Phys. Rev. B* **79**, 224511 (2009).
- ⁴⁴ C. H. Lee, K. Kihou, H. Kawano-Furukawa, T. Saito, A. Iyo, H. Eisaki, H. Fukazawa, Y. Kohori, K. Suzuki, H. Usui, K. Kuroki, and K. Yamada, *Phys. Rev. Lett.* **106**, 067003 (2011).
- ⁴⁵ K. Suzuki, H. Usui, and K. Kuroki, *Phys. Rev. B* **84**, 144514 (2011).
- ⁴⁶ J.T. Park *et al.*, *Phys. Rev. B* **82**, 134503 (2010).
- ⁴⁷ J.T. Park *et al.*, *Phys. Rev. Lett.* **107**, 177005 (2011).
- ⁴⁸ T. Maier *et al.*, *Phys. Rev. B* **83**, 100515(R) (2011).
- ⁴⁹ Bad nesting of the Fermi surface does not necessarily imply low T_c . In fact, the nesting between electron and hole Fermi surfaces is not so good in the system studied by K. Kuroki and R. Arita in *Phys. Rev. B* **64**, 024501 (2001) (see Fig.4 of this paper), where a possibility of high T_c superconductivity originating from disconnected Fermi surfaces was proposed.